RED LESION DETECTION USING REGION BASED METHOD AND DSFs FOR RETINOPATHY SCREENING

Dr.S.G.Hymlin Rose, Assistant Professor, Departmentof ECE, R.M.D Engineering College, Chennai, hymlinrose@gmail.com

Dr.S.Janani, Associate Professor, Department of ECE, Periyar Maniammai Institute of Science and Technology, Thanjavur, drsjananiece@gmail.com

Abstract

Reliable detection of retinal lesions in fundus images is required for the creation of an automatic telemedicine system for computer-aided screening and grading of diabetic retinopathy. Propose an automatic approach for detecting microaneurysms and haemorrhages in retina pictures in this project. The most common and often the first lesions to occur as a result of diabetic retinopathy are microaneurysms and haemorrhages. As a result, their detection is required for both pathology screening and follow-up (progression measurement). This task, which is now done by hand, may be automated to improve objectivity and reproducibility. Previous approaches for detecting red lesions in retinal pictures failed to perform consistently across all regions. As a result, reliable detection of lesions in all parts of pictures remains a challenge. Consider the region in your suggested work. Consider region-based segmentation with previous DSF analysis in the suggested study. Red lesions are recognised in this way so that they may be graded simply. It is accomplished by splitting the retinal picture into separate zones in accordance with international standards. This approach adapts the search region for red lesion detection to the image size. Erosion and dilation are used to remove OD and vessels from the resulting image region by region. Finally, a hybrid kernel SVM classifier is used to distinguish between lesion and non-lesion cases. As a result, the sensitivity, specificity, and accuracy of the system can be increased.

Keywords:fundus, haemorrhage,retinopathy

DOINumber:10.14704/nq.2022.20.8.NQ44632 **NeuroQuantology2022;20(8):6062-6074**

INTRODUCTION

Early detection of diabetic retinopathy, as well as appropriate treatment, has been found to reduce the risk of vision loss and blindness. This is notably beneficial in diabetic screening programmes run by various countries, when hundreds of people are checked using images acquired with a fundus camera from both eyes. Given the large number of diabetic patients screened each year, the number of retinal images generated is large, and the majority of them are normal (typically, over 90% do not show any signs of diabetic retinopathy), so an automatic means of discarding the patients without abnormalities can significantly reduce the workload of doctors while also improving the quality of life of diabetic patients.

Diabetic retinopathy is a disorder that affects vision by developing cataracts, glaucoma, and, most significantly, damage to blood vessels inside the eye. Diabetic retinopathy is a diabetic condition caused by alterations in the retina's blood vessels. The retina's blood vessels are then broken, leaking blood and sprouting frail brush-like branches and scar tissue. The vision images that the retina provides to the brain may be blurred or

distorted as a result of this. In the United States, diabetic eye disease is the primary cause of blindness. People with untreated diabetes are reported to be 25 times more likely than the average population to become blind. Diabetic retinopathy is more likely to develop as a person's diabetes progresses. The frequency of serious vision loss has been considerably reduced thanks to regular, thorough eye care and treatment when necessary. Your ophthalmologist can help you avoid major visual problems if you have diabetes.

Diabetic retinopathy usually doesn't cause any symptoms unless the damage to your eyes is severe. Blurred vision and gradual vision loss are symptoms of diabetic retinopathy. Floaters, shadows, or missing visual patches, and difficulty seeing at night Before serious eye bleeding begins, many persons with early diabetic retinopathy have no symptoms. For further processing, vascular tree segmentation from the background is required for vessel assessment. The position of blood vessels can be used to limit the amount of false positives in the identification of micro aneurysms and haemorrhages.

Digital colour fundus photography allows for the non-invasive capture of fundus images, which is required for large-scale screening. The quantity of fundus images that need to be inspected by ophthalmologists in a diabetic retinopathy screening program can be unreasonably huge. In a screening scenario, the number of photographs without any sign of diabetic retinopathy is often over 90%. As a result, an automated system that can determine whether or not an image has any symptoms suspicious for diabetic retinopathy might improve efficiency; only those photos judged suspect by the system would require ophthalmologist evaluation. Red lesions, such as microaneurysms and intraretinalhaemorrhages, and white lesions, such as exudates and cottonwool patches, are signs of diabetic retinopathy. This study only looks at red lesions, which are one of the earliest clear indications of diabetic retinopathy.

As a result, detecting them is crucial for a pre-screening system. Diabetic retinopathy is classified morphologically based on the number, location, and type of distinct microvascular lesions found in the fundus of the eye. 1 Because of the difficulty of the task, the chronological sequence of appearance, maturation, and elimination of fundus lesions is not accounted for in the analysis. An exact lesion count may be employed for low lesion densities, but no attempts at counting are performed for greater lesion densities. Instead, a semiquantitative classification is achieved by comparing standard pictures taken at various stages of retinopathy.

Digital analysis of fundus photographic pictures may allow for comprehensive lesion mapping and counting, as well as dynamic analysis of fundus photograph time series. The most basic automatable task of practical utility is probably discriminating between people without retinopathy and those with any level of retinopathy, with the latter requiring secondary-level evaluation: in this case, a visual evaluation by an ophthalmologist or a grader. In populations undergoing photographic screening, the absence of retinopathy is identified in a substantial majority of diabetic patients. 2 Because it may need comprehensive analysis of borderline aspects of questionable identity, diagnosing the absence of retinopathy or the presence of a single or very few lesions takes longer than diagnosing low levels of retinopathy.

The goal of this project is to create an automated approach for detecting red lesions in photos with a high sensitivity and a reasonable specificity. This enables the approach to be utilised as part of a pre-screening process. In three steps, we solve the challenge of detecting red-lesions. Each image is first preprocessed; after that, candidate objects that could represent red-lesions are extracted; and finally, the chance of each candidate representing a red-lesion is calculated using a classifier and a vast set of specially constructed characteristics.

The system is fine-tuned and trained on a set of 50 images that are representative of

those used in a screening environment, then tested on a separate set of 50 photographs. To give a reference standard, an experienced ophthalmologist painstakingly identified all red-lesions in these photos. To facilitate comparison between the automatic systems' and human performance, a second experienced ophthalmologist indicated all red-lesions in the test set.

The project's goal is to develop a method for automatically detecting haemorrhages and microaneurysms in digitised fundus photographic images of diabetic retinopathy patients, as well as to compare automated detection to visual identification of diabetic retinopathy. It also aims to improve detection accuracy by red lesion features and distinguish genuine red lesions from artefacts.

RELATED WORK

'Retinal Imaging and Image Analysis' by M.D. Abramoff was published in 2010. Deals with features of picture acquisition, image analysis, and clinical significance, all of which are discussed together because of their mutually interconnected nature. Furthermore, digital imaging has the advantages of easier storage on media that do not degrade in quality over time, the ability to transmit images over short distances within a clinic or over large distances via electronic transfer (allowing expert "at-a-distance" opinion in large rural communities), the ability to process images to improve image quality, and the potential for automated diagnosis. Large databases of fundal images can be automatically categorized and managed more easily in the research or screening scenario than labor-intensive observer-driven procedures. Automated diagnosis may also aid decision-making for optometrists.

A novel approach for diagnosis and severity grading of diabetic maculopathy was reported by Roychowdhury.S (2013). This research describes an automated technique for detecting maculopathy and rating its severity. The fovea region is located by detecting the centre of the optic disc and using the superior and inferior vascular arcades within the retina. The macular regions are subsequently graded according to an international grading system. Following that, morphological approaches are used to detect lesions in scaled macular regions. For the severity grading of maculopathy into normal, mild, moderate, and severe, features are identified and selected, then fed to the multiclass SVM. The proposed method was tested on publicly available databases and achieved a sensitivity of 96.89% and a specificity of 97.15% which is really competitive with the state-of-the-art in this area.

A presentation titled 'An Ensemble Classification-Based Approach Applied to Retinal Blood Vessel Segmentation' was given by Fraz M.M. in 2012. A new supervised method for segmenting blood vessels in retinal pictures is presented in this research. This method employs a feature vector based on gradient vector field orientation analysis, morphological transformation, line strength measures, and Gabor filter responses, as well as an ensemble system of bagged and boosted decision trees. The ensemble system's performance is examined in depth, and the algorithm's resulting accuracy, speed, resilience, and simplicity make it an ideal tool for automated retinal image processing.

Marin.D (2014) delivered a paper titled "Automatic and Efficient Fovea Center Detection in Retinal Images." The detection of the MF (macula fovea) centre in retinal pictures is provided in a fast and automated manner, which is required for the DR (diabetic retinopathy) screening project or the computer aided diagnosis of DME (diabetic macular edema). The method is based on the limits imposed by preexisting retinal anatomical structures on relative positions and intensity information within the OD (optic disc) circle boundary. To begin, adaptive thresholding, morphological bottom-hat transform, and region-based active contour model techniques are used to precisely determine the OD circle border. After that, the fovea region is chosen by examining the OD's intensity information. Finally, mathematical morphology is used to detect the MF centre. The key advantage of the

presented approach is that it takes only roughly 12 seconds per image because it does not rely on blood vessel segmentation in advance. The experimental results indicate that the method has the potential to outperform equivalent methods provided in other literatures.

Automatic detection of microaneurysms and haemorrhages in fundus images using dynamic shapefeatures' was given by Lama Seoud (2014). This research proposes a novel method for detecting microaneurysms and haemorrhages in fundus pictures automatically. It starts with a shade correction, contrast enhancement, and denoising preprocessing stage. Second, candidates are selected from all regional minima with appropriate contrast. Third, a new set of dynamic form features is generated as a function of intensity in an image flooding technique. Finally, the candidates are classified as lesions or non-lesions using a Random Forest. For training and testing, a series of 143 fundus pictures with an average diameter of 2210 pixels was obtained using various cameras. The suggested method gets a global score of 0.393 across the FROC curve, whereas previous work with similar resolution photos yielded a score of 0.233.

Most of the existing retinal segmentation methodologies are evaluated on the healthy retinal images free from the pathologies; therefore, their performance can be considerably degraded in the presence of lesions.

PROPOSED SYSTEM

Because the majority of existing retinal segmentation approaches are tested on healthy retinal images free of diseases, their performance can be significantly harmed in the presence of lesions. In this study, region-based segmentation is proposed as a method for accurately detecting the lesion. It is accomplished by splitting the retinal picture into separate zones in accordance with international standards. This approach adapts the search region for red lesion detection to the image size. Erosion and dilation are used to remove OD and vessels from the resulting image region by region. Microaneurysms and haemorrhagesare both identified in this area.

For each candidate, dynamic form features and colour features are extracted. The hybrid kernel SVM classifier is used to distinguish between lesion and non-lesion cases. Hyperplane achieves all feasible separation of point set in hybrid kernel SVM classifier. Two steps are employed in the SVM classifier. There are two phases: training and testing. For accurate red lesion detection, the training and testing stages are separated by a hyperplane.

PROPOSED SYSTEM ARCHITECTURE

The original fundus image is taking as input mage .The main steps in proposed system are

1) Spatial calibration
2) Image Preprocessing
3) Region based segmentation
4) Vessels and optic disc removal
5) Dynamic Shape Features
6) Classification

The filter used in proposed system is the mean filter. Here the vessels and lesions are detected region wise using region based segmentation. The classifier used here is the hybrid SVM classifier.

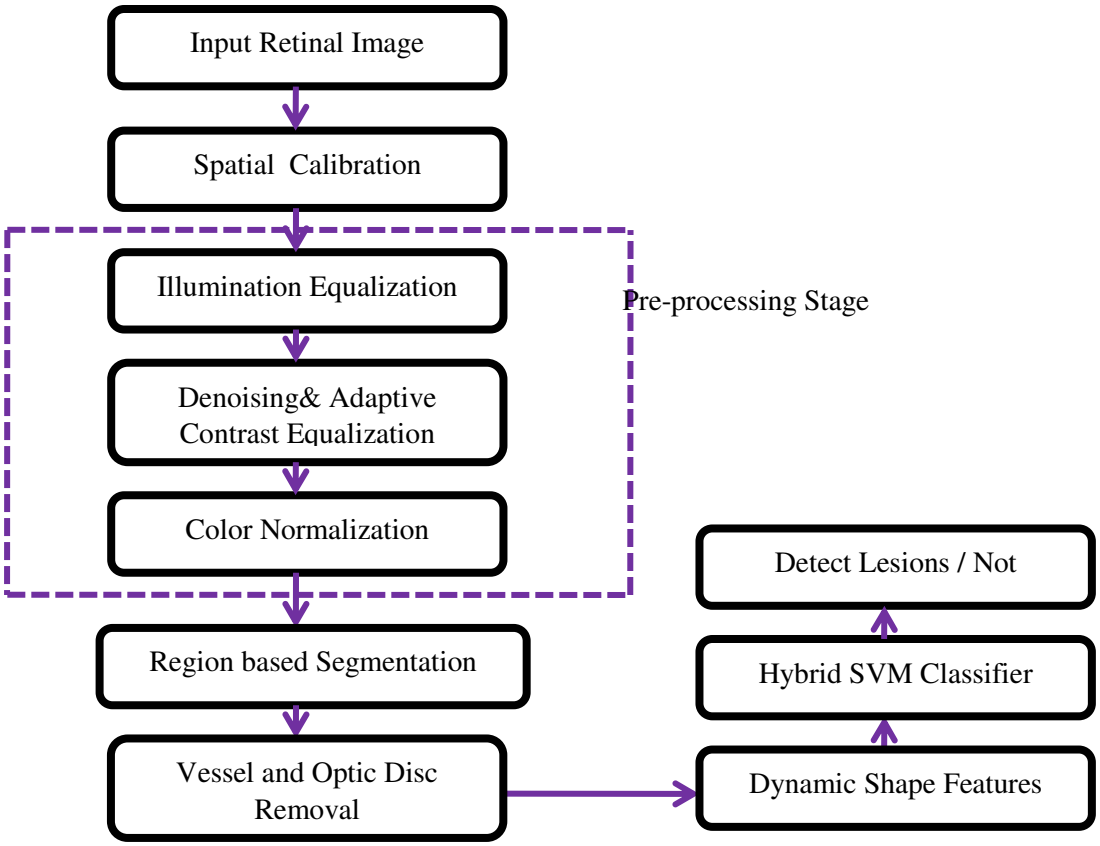

Figure 3.1 .Block diagram of proposed system

3.4.1 Spatial Calibration

To adapt to different image resolutions, we use a spatial calibration method introduced. Images are not resized. Rather, the diameter of the ROI (after removal of the dark background) is taken as a size invariant. This hypothesis is reasonable since most of the images for DR screening are acquired with a field of view (FOV) of 45°. D is used to set the kernel sizes of the different filters in the proposed method.

Three size parameters are used in our method:

- d_1 is the average radius of the OD
- d_2 is the size of the smallest MA
- d_3 is the size of the largest HE

In the case of eye fundus images obtained with a FOV of 45°, we have experimentally set these parameters to d1=D/10; d2=D/360 and d3=D/28.

3.4.2 Image Pre-processing

The illumination of the retina is often nonuniform, leading to local luminosity and contrast variation. Lesions may be hardly visible in areas of poor contrast and/or low brightness. Moreover, in a telemedicine context, images are variable in terms of color and quality. Consequently, pre-processing steps are required to address these issues. The successive steps are detailed hereafter.

A) Illumination Equalization:

To overcome the vignetting effect, the illumination equalization method is used:

$$I_{ie} = I + \mu - I * h_{m1} \quad (3.1)$$

A large mean filter (h_{M1}) of diameter $d_1$is applied to each color component of the original image I in order to estimate its illumination.

Then, the resulting color image is subtracted from the original one to correct for potential shade variations. Finally, the average intensity μ of the original channel is added to keep the same color range as in the original image.

B) Denoising:

A small mean filter (h_{M2}) of diameter $d_2$is applied to each color channel of the resulting

image in order to attenuate the noise resulting from the acquisition and compression steps without smoothing the lesions.

C) Adaptive Contrast Equalization:

The contrast drift is approximated using the local standard deviation computed for each pixel in a neighborhood of diameter d_1 for each color channel (I_{std}) . Areas with low standard deviation indicate either low contrast or smooth background. To enhance low contrast areas, we sharpen the details in these specific regions using for each color channel separately:

$$I_{ce} = I_{dn} + \frac{1}{I_{std}}(I_{dn} * (1 - h_{m3}))..\ (3.2)$$

Local image details are thereby added to the denoised image, weighted by the inverse of the contrast drift. The details are obtained using a high pass filter, derived from a mean filter (h_{M3}) of diameter d_3. The previous denoising step prevents undesirable noise sharpening

.**D) Color Normalization**

Color normalization is necessary in order to obtain images with a standardized color range. We perform, in each color channel of I_{ce}, histogram stretching and clipping in the range μ+3σ, where μ and σ are the mean and standard deviation of the color channel in the ROI.

3.4.3 Optic Disc Removal

The OD is a significant source of false positives in red lesion detection therefore its removal is a necessary step. Starting from the preprocessed image, we first use an entropy-based approach to estimate the location of the OD's center. Basically, the OD is located in a high intensity region where the vessels have maximal directional entropy. A subsequent optimization step then estimates the OD's radius and refines its position. This consistsin convolving a multi-scalering-shaped matched filter to the image in a sub-ROI centered on the first estimation of the OD's center, of radius equal to a third of the ROI's radius. The radius and position of the matched filter that minimizes the convolution are selected as the OD's final radius and center position.

3.4.4 Candidate Extraction

Since blood vessels and dark lesions have the highest contrast in the green channel the latter is extracted from the preprocessed image and is denoted G_p . The red and blue channels are used later to extract color features. In the green channel,

MAs and HEs appear as structures with local minimal intensity. A brute force approach would be to extract all the regional minima in.

A regional minimum is a group of connected pixels of constant intensity, such that all the adjacent pixels have strictly higher intensities

. Unfortunately, this method is highly sensitive to noise. Depending on the smoothness of the image, the number of regional minima can thus be very large. To overcome this limitation, we adopt the dynamics transformation which rates regional minima according to their local contrast.

Noisy minima usually have lower contrast than red lesions. In a topographic representation of G_p, the dynamic of a minimum is computed as the difference in intensity between the given minimum and the brightest points of the paths reaching a minimum of lower intensity. The main advantage of this definition is that the resulting contrast measurement is independent of the size and shape of the regional minimum.

Using this transformation, we can select the minima by thresholding the resulting contrast image. At this point, we would like to discard from the set of candidates as many local minima corresponding to noise as possible. In order to estimate the noise's intensity, we compute the local standard deviation in a neighborhood of the size of the papilla and consider the lowest standard deviation inside the ROI, which would correspond to a region in the retinal background with minimal signal intensity.

Finally, a selected minimum should have intensity lower than the mean intensity in to be considered a candidate region. This is

supported by the fact that we are looking for red lesions, which are darker than the retinal background. Contrast and illumination equalization gain are importance at this point. Without these preprocessing steps, global contrast and intensity thresholding would be difficult to achieve.

In addition, all candidates whose distance to the OD's center is smaller than the OD's radius are removed from the set of candidates and not considered any further.

3.4.5 Region based Segmentation

In proposed algorithm region of interest is adaptive to the size of image. Firstly the centre of the actual image is find by using its mask.

From centre of retinal the image is divided into different region to classify between lesions and non-lesions. Image is divided into four regions to describe the severity of red lesion. Region division covered whole image, so lesions are detected in every region of image. Optic disc is also detected region wise and unwanted artifacts are successfully removed.

Algorithm: Region classification

1. Region 1:From(xm,ym) a circular region is obtained of radius (y/10)
2. Region2: From(xm,ym) a circular region is obtained of radius 2*(y/10) – Region1
3. Region3:From (xm,ym) region is obtained of radius 3*(y/10)- (Region1+Region2) 4. Region 4: Image-(Region 1+ Region 2+Region 3)

Extract and Remove

Extraction and removal of unwanted artifacts (OD and vessels) in resultant image is also applied region wise. As region 1 does not consists optic disc and vessels, so region 1 is not considered for these operations of extraction and removal of unwanted artifacts. This will save some computation load of the method. Optic disc is detected by using mean and standard deviation of region of an image as described as follows.

1. Convert selected RGB region (R) into gray image (RG)

2. Calculate mean and standard deviation of (RG)

3. I=R-(mean(RG) + std (RG))

4. I1=I- mean(RG)

5. Convert into binary image

6. Select maximum area

Vessels are extracted using green channel of regions by applying image reconstruction by using erosion and dilation. These unwanted parts are removed from resultant image of hard exudates by applying XOR operation between resultant image and image having optic disc or vessels. Then remove the OD and vessels.

3.4.6 Dynamic Shape Features

Among the candidates, several regions correspond to non-lesions, such as vessel segments and remaining noise in the retinal background. To discriminate between these false positives and true lesions, an original set of features, the DSFs, mainly based on shape information, is proposed. In a topographic representation of G_p, each candidate corresponds (by analogy) to a water source, denoted. Morphological flooding is applied to starting from the lowest water source and ending when the retinal background is reached.

It is indeed hypothesized that when the flooding reaches the retinal background intensity, the catchment basins degenerate and no longer contextually represent a red lesion.

At each flooding level, pixels that are adjacent to a water source and lower than the flooding level are added to the catchment basin of S_j, denoted B^{Sj}. When two basins merge, they start sharing the same pixels and thus the same attributes. We implement the image flooding using hierarchical queues.

At each flooding level, for each candidate, six shape attributes are computed on the catchment basin:

- **Relative area:** number of pixels in , divided by the total number of pixels in the ROI.
- **Elongation: 1-W/L** with W and L the width and length, respectively, of the bounding box of oriented along its major axis.
- **Eccentricity:** W and L the width and length, respectively, of the bounding box of oriented along its major axis

$\sqrt{(L^2 - W^2)/L^2}$ ... .(3.3)

- **Circularity:** ratio of the area of over its squared perimeter and multiplied by 4π.
- **Rectangularity:** ratio of the area of over the area of its bounding box oriented along its major axis.
- **Solidity:** ratio of the area of over the area of its convex hull. Six curves are obtained for each candidate, one per shape attribute and as a function of the flooding level.

A linear least-squares regression is performed on each curve. Depending on the order of the fit, the number of regression parameters is equal to K +1. These parameters and the root mean squared error of the fit constitute the first features. The last 2 features are the mean and median values over the flooding levels. In total, DSFs are computed for each candidate. Candidates and correspond to vessel segments, being on a relatively large segment while is part of a third order segment close to the fovea. Candidate corresponds to a medium HE, and candidate to a MA. The mean intensity of the image is equal to 110 in this example.

Each evolving layer encompasses the previous ones. At each level, the shape features, for example and , are computed on the catchment basins and reported on the graph of together with their order linear fit. The elongation function reveals that candidates and evolve in a more elongated manner than candidates, with larger values for their linear fit intercepts. Indeed, the catchment basins of these vessel segments extend anisotropically, following the direction of the vessel. By contrast, the circularity functions reveal that candidates and evolve toward a more circular shape, with positive slopes, particularly for candidate which corresponds to a MA. Finally, the solidity function reveals that at intensity level 40 for candidate, the catchment basin appears to merge with the rest of the vasculature and drops in solidity with a negative slope.

The same goes for candidate but at a higher intensity level (100) since it is part of a much smaller and contrasted vessel than S_1. The solidities of candidates, however, either increase (positive slope) for the HE, or stay constant and high (slope close to zero and intercept of almost 100) for the MA, indicating that these structures are isolated from the other catchment basins. Four more features, computed on the local minima, are added to the features vector: the mean red, green and blue values in and the local contrast in G*p*

3.4.7 Classification

To distinguish between lesions and non-lesions, use a hybrid RBF Kernel SVM classifier. It is robust against outliers and over-fitting. There are two phases in the SVM .They are

1. Training phase
2. Testing phase.

The output from the DSFs is given as input to the training phase. Here , all the possible separations of the point set can be achieved by a hyper plane. In the Lagrange optimization formulation can find the optimal separating hyper plane normal vector.

Advantages of proposed system.

- Low computational complexity
- Higher accuracy of identification.
- Reduce the number of pixels under classification
- The improved performance in terms of sensitivity, specificity and accuracy
- Robust features and highly capable of discriminating between lesions and vessel segments

Experimental reuslts

Color fundus image gives the background image of eye. The fundus image is taken by fundus camera. Below figure 4.1 shows the original fundus image. To adapt different image resolution the large mean filter is applied to the original image. Below fig.4.2 shows the simulation result of spatial calibration

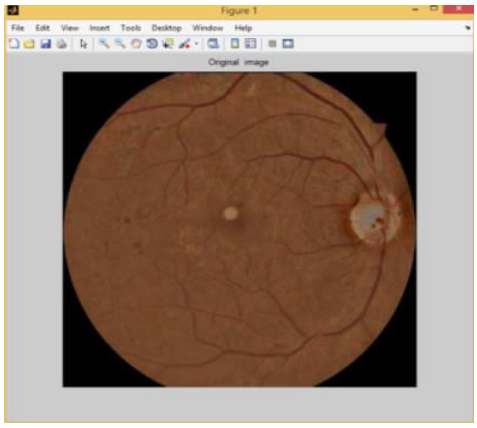

Figure.4.1.Original Fundus Image

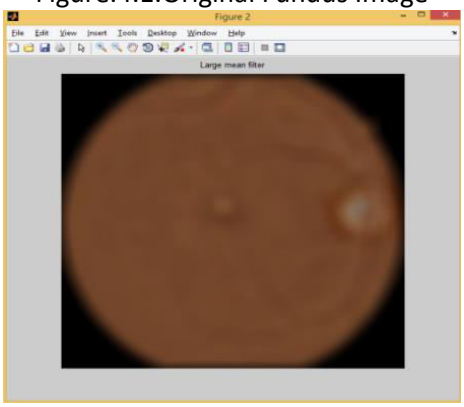

Figure.4.2.Spatial calibration

In image pre-processing, illumination Equalization is the first stage. To avoid vignetting effect illumination Equalization is done. Below figure 4.3 shows the output of illumination equalization. Adaptive contrast equalization is the second stage in image preprocessing. It is done to enhance the low contrast areas. Below figure 4.4 shows the output of adaptive contrast equalization

Figure.4.3.Illumination Equalization

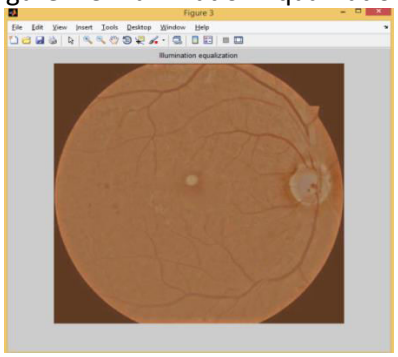

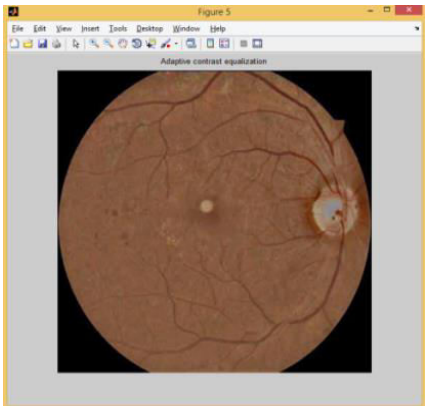

Figure.4.4. Adaptive Contrast Equalization

Color normalization technique is used to get the standardized color range of the image. Below fig 4.5 shows the output of color normalization. Blood vessels and dark lesion have highest contract in green channel, so in candidate extraction the green channel image is used. Below figure 4.6 shows the green channel image.

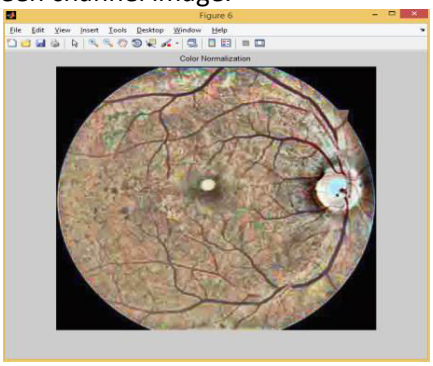

Figure.4.5.Color Normalization

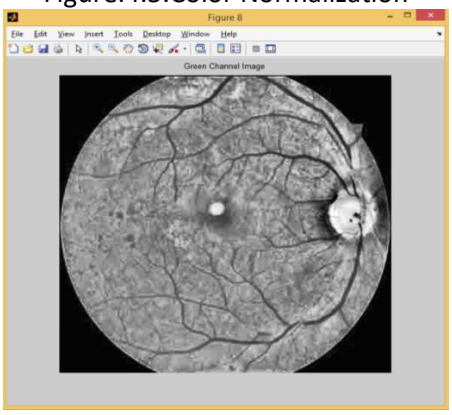

Figure.4.6.Green Channel Image

Optic disc removal is the essential one, because it is the source of false positives in red lesion detection. The location of optic disc is estimated using mean and standard deviation

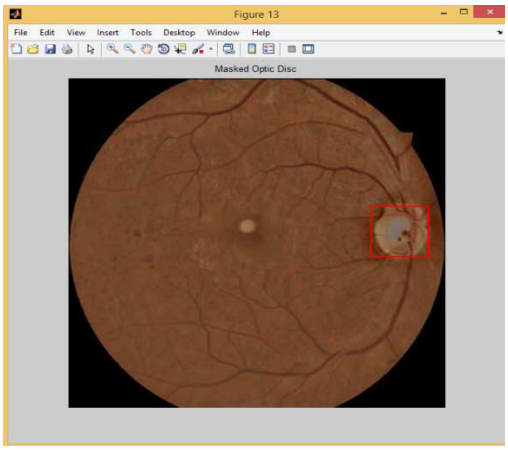

Figure.4.7.Region Based Segmentation

Region 1, it is obtained of radius (y/10). Region2 is obtained of radius 2*(y/10)–(region1). Region 3 is obtained of 3*(y/10)-(region1+region2). Below figure 4.8 shows the simulation results of divided regions.

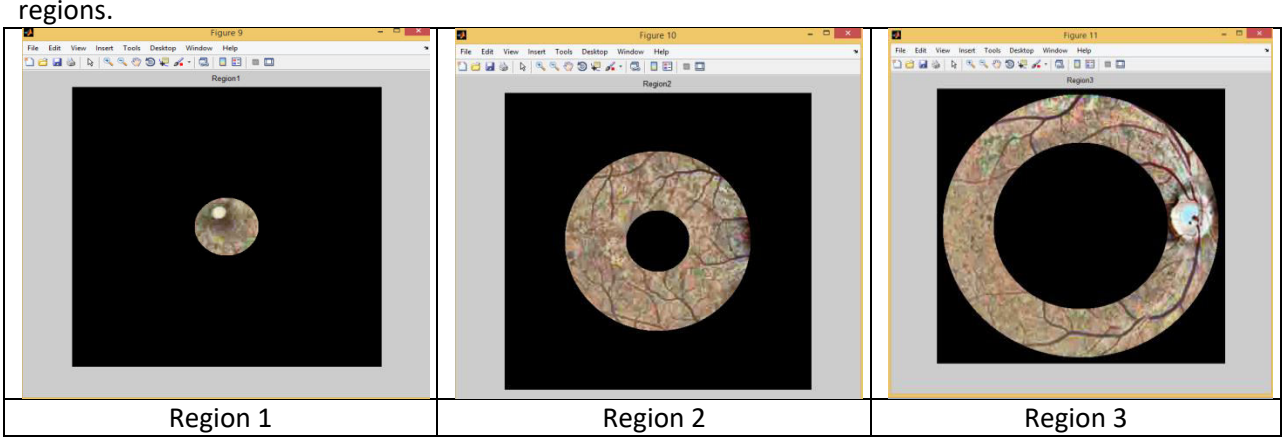

Region 1	Region 2	Region 3

Figure4.8. Simulation result of divided region

Normal red lesion detection

Normal red lesion detection is the manual detection of red lesion. In normal red lesion detection the blood vessels are detected as red lesion. Below fig 4.11 shows the simulation result of normal red lesion detection.

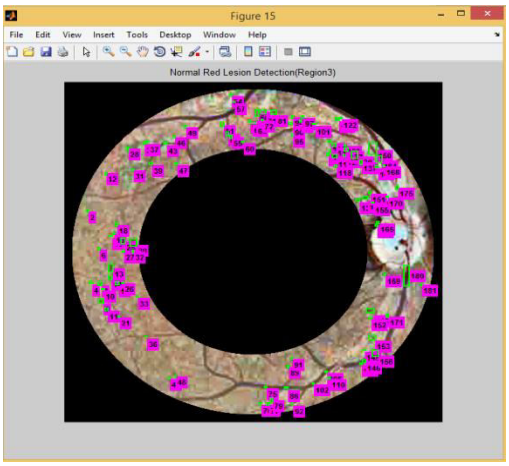

Figure.4.9 Normal red lesion detection

The original red lesion are obtained after applying the dynamic shape features and hybrid SVM classification .Below fig.4.12 shows the final red lesion detection.

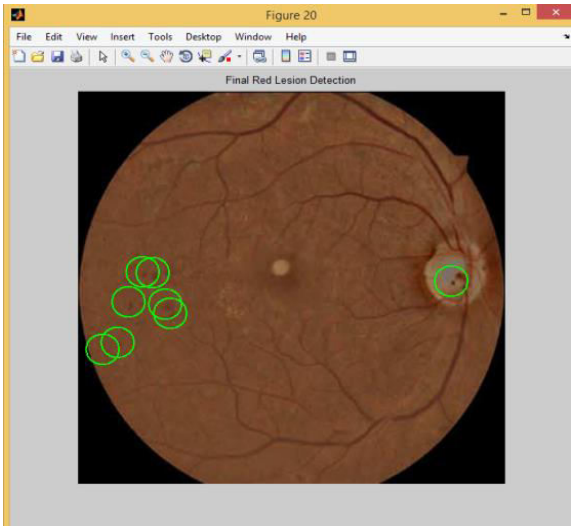

Figure 4.10. Final red lesion detection output

DISCUSSION

The results of our experiments indicate that the DSFs combined with the proposed pre-processing steps are highly discriminated. The main advantage of these shape features is that no precise prior segmentation of the candidates is needed since feature computation is performed at different levels throughout the image flooding. Even on the highly heterogeneous dataset, the proposed method achieves satisfactory results, proving its robustness with respect to differences in image resolution and retina camera. Compared to our previous paper evaluated on the same dataset, the addition of the adaptive contrast equalization allows the detection of more lesions located in poorly contrasted areas that were otherwise lost at the candidate extraction step. Nevertheless, the proposed method yields a sensitivity lower than that of human experts for the same FPI rate.

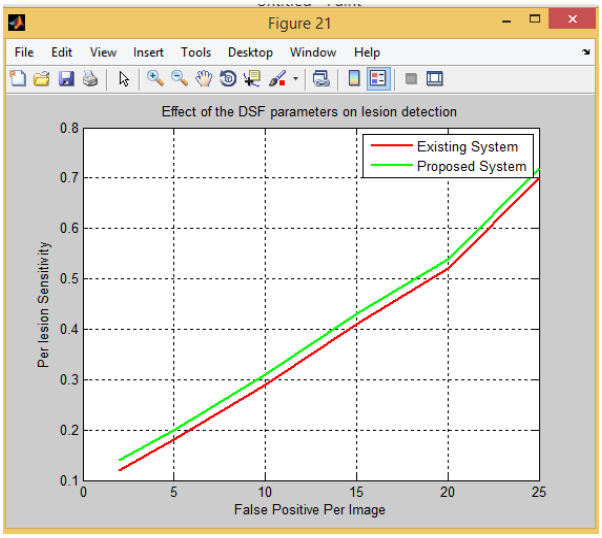

Figure 4.11 Effect of DSF parameters on lesion detection

CONCLUSION

A novel red lesion detection method based on a new set of shape features, the DSFs, was presented and evaluated on six different databases. The results demonstrate the strong performance of the proposed method in detecting both MAs and HEs in fundus images of different resolution and quality and from different acquisition systems. The method outperforms many state-of-the-art approaches at both per-lesion and per-image levels. DSFs have proven to be robust features, highly capable of discriminating between lesions and vessel segments. The concept of DSFs could be exploited in other applications, particularly when the objects to be detected do not show clear boundaries and are difficult to segment precisely. Here the region based segmentation was performed so the red lesion are detected region wise .Thus the performance of detecting red lesion is improved in terms of accuracy ,sensitivity and specificity. Further work focusing on bright lesion and neo vessel

detection will complete the proposed system and allow automatic DR grading.

REFERENCES

[1] J. T. Barron and J. Malik, "Shape, illumination, and reflectance from shading," IEEE Transactions on Pattern Analysis and Machine Intelligence, vol. 37, no. 8, pp. 1670–1687, 2015.

[2] H. Barrow and J. Tenenbaum, "Recovering intrinsic scene characteristics," Comput. Vis. Syst., A Hanson & E. Riseman (Eds.), pp. 3–26, 1978.

[3] S. Bell, K. Bala, and N. Snavely, "Intrinsic images in the wild," ACM Transactions on Graphics (TOG), vol. 33, no. 4, p. 159, 2014.

[4] X. Fu, Y. Sun, M. LiWang, Y. Huang, X.-P. Zhang, and X. Ding, "A novel retinex based approach for image enhancement with illumination adjustment," in 2014 IEEE International Conference on Acoustics, Speech and Signal Processing (ICASSP). IEEE, 2014, pp. 1190–1194.

[5] X. Fu, Y. Liao, D. Zeng, Y. Huang, X.-P. Zhang, and X. Ding, "A probabilistic method for image enhancement with simultaneous illumination and reflectance estimation," IEEE Transactions on Image Processing, vol. 24, no. 12, pp. 4965–4977, 2015.

[6] B. V. Funt, M. S. Drew, and M. Brockington, "Recovering shading from color images," in European Conference on Computer Vision. Springer, 1992, pp. 124–132.

[7] E. Garces, A. Munoz, J. Lopez-Moreno, and D. Gutierrez, "Intrinsic images by clustering," in Computer graphics forum, vol. 31, no. 4. Wiley Online Library, 2012, pp. 1415–1424.

[8] R. Grosse, M. K. Johnson, E. H. Adelson, and W. T. Freeman, "Ground truth dataset and baseline evaluations for intrinsic image algorithms," in Computer Vision, 2009 IEEE 12th International Conference on. IEEE, 2009, pp. 2335–2342.

[9] K. Gu, G. Zhai, X. Yang, W. Zhang, and C. W. Chen, "Automatic contrast enhancement technology with saliency preservation," IEEE Transactions on Circuits and Systems for Video Technology, vol. 25, no. 9, pp. 1480–1494, 2015.

[10] M. Herscovitz and O. Yadid-Pecht, "A modified multi scale retinex algorithm with an improved global impression of brightness for wide dynamic range pictures," Machine Vision and Applications, vol. 15, no. 4, pp. 220–228, 2004.

[11] H. Ibrahim and N. S. P. Kong, "Brightness preserving dynamic histogram equalization for image contrast enhancement," IEEE Transactions on Consumer Electronics, vol. 53, no. 4, pp. 1752–1758, 2007.

[12] D. Menotti, L. Najman, J. Facon, and A. d. A. Ara´ujo, "Multi-histogram equalization methods for contrast enhancement and brightness preserving," IEEE Transactions on Consumer Electronics, vol. 53, no. 3, pp. 1186–1194, 2007.

[13] D. J. Jobson, Z.-u. Rahman, and G. A. Woodell, "Properties and performance of a center/surround retinex," IEEE transactions on image processing, vol. 6, no. 3, pp. 451–462, 1997.

[14] R. Kimmel, M. Elad, D. Shaked, R. Keshet, and I. Sobel, "A variational framework for retinex," International Journal of Computer Vision, vol. 52, no. 1, pp. 7–23, 2003.

[15] E. H. Land and J. J. McCann, "Lightness and retinex theory," JOSA, vol. 61, no. 1, pp. 1–11, 1971.

[16] Y. Li and M. S. Brown, "Single image layer separation using relative smoothness," in Proceedings of the IEEE Conference on Computer Vision and Pattern Recognition, 2014, pp. 2752–2759.

[17] Z. Liang, W. Liu, and R. Yao, "Contrast enhancement by nonlinear diffusion filtering," IEEE Transactions on Image Processing, vol. 25, no. 2, pp. 673–686, 2016.

[18] J. M. Morel, A. B. Petro, and C. Sbert, "A pde formalization of retinex theory," IEEE Transactions on Image Processing, vol. 19, no. 11, pp. 2825–2837, 2010.

[19] M. K. Ng and W. Wang, "A total variation model for retinex," SIAM Journal on

Imaging Sciences, vol. 4, no. 1, pp. 345–365, 2011.

[20]Z. Rahman, D. J. Jobson, and G. A. Woodell, "Retinex processing for automatic image enhancement," Journal of Electronic Imaging, vol. 13, no. 1, pp. 100–110, 2004.

[21]A. M. Reza, "Realization of the contrast limited adaptive histogram equalization (clahe) for real-time image enhancement," Journal of VLSI signal processing systems for signal, image and video technology, vol. 38, no. 1, pp. 35–44, 2004.

[22]Robertson, "A multiscale retinex for bridging the gap between color images and the human observation of scenes," IEEE Transactions on Image processing, vol. 6, no. 7, pp. 965–976, 1997.

[23]H. Sawant and M. Deore, "A comprehensive review of image enhancement techniques," International Journal of Computer Technology and Electronics Engineering (IJCTEE), vol. 1, no. 2, pp. 39–44, 2010.

[24]J. Shen, X. Yang, X. Li, and Y. Jia, "Intrinsic image decomposition using optimization and user scribbles," IEEE Transactions on Cybernetics, vol. 43, no. 2, pp. 425–436, 2013.

[25]C. Xiao and Z. Shi, "Adaptive bilateral filtering and its application in retinex image enhancement," in Image and Graphics (ICIG), 2013 Seventh International Conference on. IEEE, 2013, pp. 45–49.

[26]S.-H. Yun, J. H. Kim, and S. Kim, "Contrast enhancement using a weighted histogram equalization," in Consumer Electronics (ICCE), 2011 IEEE International Conference on. IEEE, 2011, pp. 203–204.

[27]C. Wang and Z. Ye, "Brightness preserving histogram equalization with maximum entropy: a variational perspective," IEEE Transactions on Consumer Electronics, vol. 51, no. 4, pp. 1326–1334, 2005.

[28]S. Wang, J. Zheng, H.-M. Hu, and B. Li, "Naturalness preserved enhancement algorithm for non-uniform illumination images," IEEE Transactions on Image Processing, vol. 22, no. 9, pp. 3538–3548, 2013.

[29]D. Zosso, G. Tran, and S. J. Osher, "Non-local retinex—a unifying framework and beyond," SIAM Journal on Imaging Sciences, vol. 8, no. 2, pp. 787–826, 2015.

*e*ISSN1303-5150